

AD-E301198

(12)

DNA-TR-81-104

AD A131149

PROPAGATION EFFECTS IN SPACE-BASED SURVEILLANCE SYSTEMS

Charles L. Rino
SRI International
333 Ravenswood Avenue
Menlo Park, California 94025

1 February 1982

Technical Report

CONTRACT No. DNA 001-81-C-0010

APPROVED FOR PUBLIC RELEASE;
DISTRIBUTION UNLIMITED.

DTIC
ELECTE
S AUG 8 1983 D
B

THIS WORK WAS SPONSORED BY THE DEFENSE NUCLEAR AGENCY
UNDER RDT&E RMSS CODE B322082466 S99QAXHA00002 H2590D.

Prepared for
Director
DEFENSE NUCLEAR AGENCY
Washington, DC 20305

DTIC FILE COPY

83 06 30 022

UNCLASSIFIED

SECURITY CLASSIFICATION OF THIS PAGE (When Data Entered)

REPORT DOCUMENTATION PAGE		READ INSTRUCTIONS BEFORE COMPLETING FORM
1. REPORT NUMBER DNA-TR-81-104	2. GOVT ACCESSION NO. AD A131 149	3. RECIPIENT'S CATALOG NUMBER
4. TITLE (and Subtitle) PROPAGATION EFFECTS IN SPACE-BASED SURVEILLANCE SYSTEMS		5. TYPE OF REPORT & PERIOD COVERED Technical Report
		6. PERFORMING ORG. REPORT NUMBER SRI Project 2394
7. AUTHOR(s) Charles L. Rino		8. CONTRACT OR GRANT NUMBER(s) DNA 001-81-C-0010
9. PERFORMING ORGANIZATION NAME AND ADDRESS SRI International 333 Ravenswood Avenue Menlo Park, California 94025		10. PROGRAM ELEMENT, PROJECT, TASK AREA & WORK UNIT NUMBERS Task S99QAXHA-00002
11. CONTROLLING OFFICE NAME AND ADDRESS Director Defense Nuclear Agency Washington, D.C. 20305		12. REPORT DATE 1 February 1982
		13. NUMBER OF PAGES 36
14. MONITORING AGENCY NAME & ADDRESS (if different from Controlling Office)		15. SECURITY CLASS (of this report) UNCLASSIFIED
		15a. DECLASSIFICATION/DOWNGRADING SCHEDULE N/A since UNCLASSIFIED
16. DISTRIBUTION STATEMENT (of this Report) Approved for public release; distribution unlimited.		
17. DISTRIBUTION STATEMENT (of the abstract entered in Block 20, if different from Report)		
18. SUPPLEMENTARY NOTES This work was sponsored by the Defense Nuclear Agency under RDT&E RMSS Code B322082466 S99QAXHA00002 H2590D.		
19. KEY WORDS (Continue on reverse side if necessary and identify by block number) Space-Based Radar Scintillation Nuclear Propagation		
20. ABSTRACT (Continue on reverse side if necessary and identify by block number) This report describes the first year's effort to investigate propaga- tion effects in space-based radars. A model was developed for analyzing the deleterious systems effects by first developing a generalized aperture distribution that ultimately can be applied to any space-based radar con- figuration. The propagation effects are characterized in terms of the SATCOM model striation parameters. The form of a generalized channel model for space-based radars is		

DD FORM 1 JAN 73 1473 EDITION OF 1 NOV 65 IS OBSOLETE

UNCLASSIFIED

SECURITY CLASSIFICATION OF THIS PAGE (When Data Entered)

UNCLASSIFIED

SECURITY CLASSIFICATION OF THIS PAGE(When Data Entered)

20. ABSTRACT (Continued)

described and the principal results are summarized. A generalized aperture model is described in both discrete and integral forms. The asymptotic form of the radar signal correlation function is derived under strong-scatter conditions. The results show that the forward and return paths are uncorrelated, which greatly simplifies the applications of the model.

To illustrate one application of the model, the average antenna pattern distortion is computed and the ramifications of such effects on the radar-signal coherence time are discussed. The SATCOM model is used to characterize the ionospheric disturbance and the attendant propagation effects.

UNCLASSIFIED

SECURITY CLASSIFICATION OF THIS PAGE(When Data Entered)

EXECUTIVE SUMMARY

Space-based radar systems have been proposed for future CONUS defense, surveillance, and tactical battle-support functions. In the initial planning of these systems, however, little attention was given to the deleterious effects of propagation disturbances, particularly in nuclear environments. To provide a means of evaluating these effects, a general propagation model based on the SATCOM formalism has been developed.

This first Topical report has been written primarily to present the mathematical details of the model. The SATCOM channel model characterizes the propagation effects in terms of a time-varying transfer function or the equivalent tap delay line for a one-way path. A radar signal traverses the disturbed region twice; moreover, the radar processor must determine the angular position of the target, which requires a high-gain antenna system.

To analyze the degradation of the antenna beam, the spatial coherence of the channel must be specified; moreover, the two-way path must be accommodated. In Section I of the report, we develop the general form of a complete radar channel model. The propagation effects are characterized by a spatially and temporally varying transfer function.

For some applications, widely dispersed array elements may be employed. In Section II, we have generalized the propagation model to accommodate angle variations over a distributed antenna aperture; however, we have not yet exercised this aspect of the model. Rather, we have concentrated our initial efforts on systems with apertures over which variations in the propagation geometry can be neglected.

A straightforward application of reciprocity shows that the signal structure of the radar echo is the product of the disturbed forward and returned complex signals. It follows, however, that the coherence function that characterizes the average structure of radar signal depends on

the fourth-order complex moment of the channel transfer function, which is not available in current SATCOM models.

We show in Section III that the forward and return paths are uncorrelated under the strong scatter conditions that are of most interest. This means that the complex signal correlation function of the radar echo is the product of the corresponding complex correlation functions for the forward and reciprocal paths, which can be derived from existing SATCOM Codes. Thus, where it is needed, the fourth-order moment can be evaluated.

To illustrate one application of the model, in Section IV we compute the average beam distortion for an idealized antenna with a Gaussian gain function. We did this so that we could analytically evaluate the integrals involved. The results of that computation confirm the following general guidelines for use of the SATCOM model to analyze radar propagation effects:

- (1) As long as the spatial coherence scale is large compared to the effective aperture size, beam distortion is negligible.
- (2) When beam distortion is negligible, the radar signal structure is simply the square of the signal structure on a one-way path.
- (3) In general, the forward and reciprocal paths differ only by the scale factor that accommodates wavefront curvature for a finite propagation distance.

These results are not strictly new. Indeed, they were incorporated, at least implicitly, in early Ballistic Missile Defense radar studies. The results, however, have not been previously developed within the framework of the SATCOM channel modeling approach.

The continuation of this effort will apply the model to simulate the degradation of satellite-borne synthetic aperture radars. Because of (3), it is only necessary to simulate a one-way path. The complete radar echo structure can be derived by appropriately scaling the signal and multiplying the results; when (2) applies, no scaling is necessary.

TABLE OF CONTENTS

<u>Section</u>	<u>Page</u>
EXECUTIVE SUMMARY	1
I INTRODUCTION	5
II PROPAGATION EFFECTS IN A DISTRIBUTED ANTENNA SYSTEM	12
III PROPAGATION EFFECTS OVER A TWO-WAY PATH	19
IV APPLICATIONS OF THE MODEL	24
REFERENCES	30

Approved	
Special Agent	
Investigator	
Supervisor	
Chief of Bureau	
Director	
For	
District	
At _____	
Special Agent	
Investigator	
Supervisor	
Chief of Bureau	
Director	
Dist _____	
Special	

LIST OF ILLUSTRATIONS

<u>Figure</u>		<u>Page</u>
1	SBR Propagation Geometry	6
2	Functional Diagram of Monostatic SBR	8
3	Coordinate System for Analysis of Distributed System	13
4	Conversion of rms Measures to Turbulent Strengths	27

I INTRODUCTION

Space-based radar (SBR) systems have been proposed for CONUS defense, surveillance, and tactical battle support functions. In the initial planning of these systems, however, very little attention was given to the effects of propagation disturbances, particularly those generated by high-altitude nuclear detonations. Thus, the objective of the research reported here is to develop an accurate, but efficient propagation model to evaluate the deleterious effects of propagation disturbances on SBR performance.

The approach we have taken follows the early work by Hardin and Tappart¹ for the SAFEGUARD system, but draws heavily on the more recent satellite communications (SATCOM) models for predicting the effects of propagation disturbances. For SATCOM, a compact channel model has been developed that characterizes the signal structure with a comparatively small number of basic parameters.² The analysis of SBR propagation effects has some unique features, however, that present SATCOM models do not accommodate.

To introduce the SBR propagation problem, consider the simple geometry shown in Figure 1. A monochromatic, spherical wave emanating from T will be distorted by any intervening structured ionization. The resultant distortion can be characterized by the complex spatial modulation function

$$h_p(C_0^+, z_p; f) \quad (1)$$

where

$$C = \frac{R_1}{R_1 + R_2} \quad , \quad (2)$$

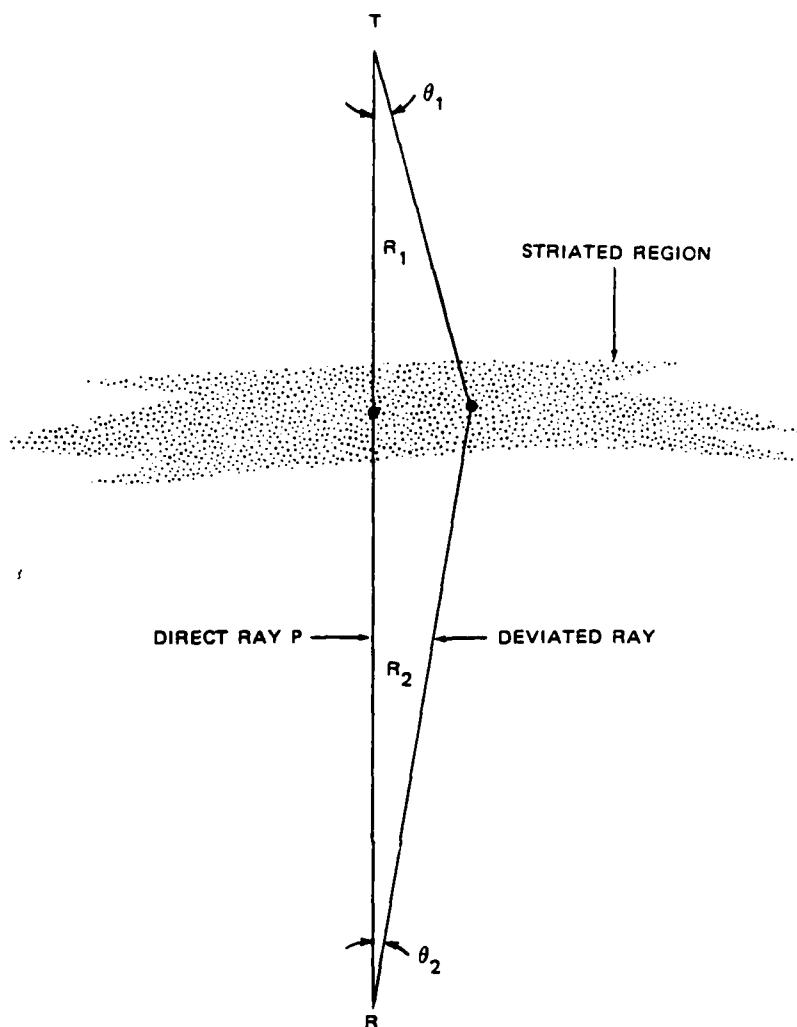


FIGURE 1 SBR PROPAGATION GEOMETRY

and

$$z_p = \frac{R_1 R_2}{R_1 + R_2} \quad (3)$$

The spatial variable $\vec{\rho}_1$ is measured perpendicular to the direct ray and f is the frequency. The subscript p is used to denote quantities that depend on the principal raypath.

Formally, $h_p(\vec{\rho}_1, z_p; f)$ is the random modulation imparted to a plane wave, as can be seen by letting R_1 approach infinity in Eqs. (2) and (3). Two correlation scales, which can be obtained from the SATCOM models, are important: (1) the spatial correlation, l_o , which is a measure of the minimum correlation distance of $h_p(\vec{\rho}_1, z_p; f)$ along $\vec{\rho}_1$, and (2) the coherence bandwidth, f_o , which is a measure of the frequency coherence of $h_p(\vec{\rho}_1, z_p; f)$.

The channel transfer function $h_p(\vec{\rho}_1, z_p; f)$ characterizes the propagation effects on a one-way path. What remains is to characterize the signals that an actual SBR system will encounter. A function diagram for a monostatic SBR is shown in Figure 2. The antenna is characterized by its aperture distribution function, $A(\vec{\rho}_1)$. The square of the spatial Fourier transform of $A(\vec{\rho}_1)$ gives the power pattern shown schematically in Figure 2.³

Similarly, the transmitted waveform can be characterized by the complex modulation function, $v_T(t)$, or its Fourier transform, $\hat{v}_T(f)$. Accommodating both the antenna and the transmitted waveform gives the general representation of the signal at R:

$$v_R(t) \propto \iint A(\vec{\rho}_1') \int h_p(C\vec{\rho}_1' + \vec{v}_E t, z_p; f + f_c) \hat{v}_T(f) \times \exp\{2\pi i f t\} df \exp\{i \Delta \vec{K} \cdot \vec{\rho}_1'\} d\vec{\rho}_1' \quad (4)$$

where v_E is the apparent transverse motion of the striations as seen from R. The vector $\Delta \vec{K}$ gives the pointing direction of the target relative to the main axis of the antenna.

The target will generate a reflected signal, which, when received at T, admits the similar representation

$$v_A(t) \propto \sqrt{G} \iint A(\vec{\rho}_1') \int h_p^R(C\vec{\rho}_1' + \vec{v}_E t, z_p; f + f_c) \hat{v}_R(f) \exp\{2\pi i f t\} df \exp\{i \Delta \vec{K} \cdot \vec{\rho}_1'\} d\vec{\rho}_1' \quad (5)$$

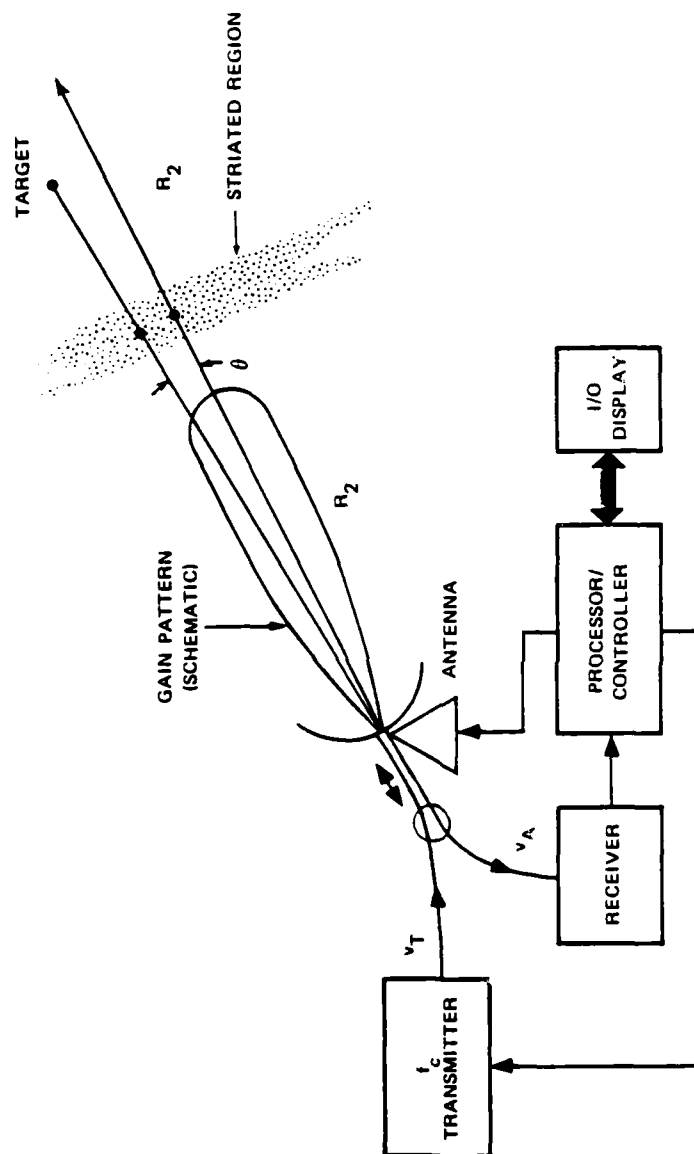


FIGURE 2 FUNCTIONAL DIAGRAM OF MONOSTATIC SBR

where

$$C^R = \frac{R_2}{R_1 + R_2} \quad (6)$$

and σ is the scattering cross section. The apparent velocity of the striations is invariant to a source-receiver interchange. Thus, the only difference in structure for the reciprocal path comes from the scale factor, C^R , which accommodates the finite distance of the signal source. Stated another way, the angular spectrum is not invariant to a source-receiver interchange, as can be deduced from Figure 1.

The SBR processor must control the transmitted waveform, the waveform repetition rate, and the antenna to detect and evaluate targets, generally in the presence of clutter and jamming. Thus, a detailed characterization of $v_A(t)$ is essential for SBR performance evaluation and the design of mitigants.

For SATCOM analyses in which only a one-way path is involved, it is comparatively straightforward to compute the signal correlation function

$$\langle v_A(t) v_A^*(t+\tau) \rangle = \mathcal{L}_c \left[\langle h_p h_p'^* \rangle \right], \quad (6)$$

which, as indicated in Eq. (6), is a function of the two-point, two-frequency correlation of the channel transfer function h_p . Under strong-scatter conditions, moreover, the signal structure can be adequately modeled by a Rayleigh process. Thus, simulations can be performed without explicit recourse to the diffraction theory.

It follows from Eqs. (4) and (5), however, that for the SBR problem

$$\langle v_A(t) v_A^*(t+\tau) \rangle = \mathcal{L}_s \left[\langle h_p h_p'^* h_p^R h_p^{R'*} \rangle \right]. \quad (7)$$

Thus, knowledge of the fourth-order moment of the channel transfer function is necessary to evaluate the second-order moment of v_A ; moreover,

\mathcal{L}_s involves a six-dimensional integration compared to a three-dimensional integration for \mathcal{L}_c . By extending our earlier analysis of the scintillation intensity structure for SATCOM, we were able to show that under strong scatter conditions

$$\langle h_p h_p^* h_p^R h_p^{R'*} \rangle = \langle h_p h_p^* \rangle \langle h_p^R h_p^{R'*} \rangle \quad (8)$$

so that

$$\langle v_A(t) v_A(t+\tau)^* \rangle = \mathcal{L}_c[\langle h_p h_p^* \rangle] \mathcal{L}_c[\langle h_p^R h_p^{R'*} \rangle] \quad (9)$$

Thus, under the strong-scatter conditions that are of primary concern, the SBR signal structure can be analyzed by running the SATCOM model for the forward and reciprocal paths and then multiply the results. Because the reciprocal path structure is simply related to the forward path, however, only one execution of the channel model algorithm is actually necessary.

If the coherence bandwidth, f_o , is larger than the signal bandwidth, Eq. (4) simplifies to

$$\begin{aligned} v_R(t) \approx v_T(t) \iint A(\vec{\rho}_1') h_p(C\vec{\rho}_1' + \vec{v}_E t, z_p; f_c) \\ \times \exp\{i\Delta\vec{K} \cdot \vec{\rho}_1'\} d\vec{\rho}_1' \quad , \end{aligned} \quad (10)$$

with a similar simplification for Eq. (5). Similarly, if the spatial coherence scale, ℓ_o , is large compared to the extent of the aperture distribution,

$$v_R(t) \approx v_T(t) g(\Delta\vec{K}) h_p(\vec{v}_E t, z_p; f_c) \quad (11)$$

where $g(\Delta\vec{K})$ is the antenna "voltage pattern." It follows that

$$v_A(t) = v_R^2(t) \quad , \quad (12)$$

which is the simplest possible case of interest.

In Section II, we present a detailed analysis of the propagation effects for a distributed antenna system. With appropriate simplifications, Eq. (10) can be recovered as a special case. The purpose of the analysis is to accommodate very large systems in which the propagation geometry can change significantly over the array. In Section III, we review the derivation of Eq. (8). In Section IV, we apply the SATCOM model and an idealized antenna system to estimate perturbation levels at which Eq. (12) becomes invalid.

To assist the reader, a notation equivalence table has been generated for the natural ionospheric models and the nuclear effects models.

II PROPAGATION EFFECTS IN A DISTRIBUTED ANTENNA SYSTEM

The model we shall consider here consists of an arbitrary configuration of noninteracting spherical wave radiators. The n^{th} element emits the spherical wave

$$\frac{\exp\{-ikr_n\}}{r_n} \quad (13)$$

An harmonic time variation is understood. Let a rectangular coordinate system be placed within the element cluster with the z axis along or near the direction of focus as shown in Figure 3.

The n^{th} array element is located by the vector, $\vec{\Delta l}_n$, in the xyz system. The field at \vec{R} is then given by the summation

$$E_R(\theta, \phi) = \sum_n A_n \frac{\exp\{i[\phi_n - kr_n]\}}{r_n} \quad (14)$$

where

$$r_n = R[1 + |\vec{\delta l}_n|^2 - 2\vec{\delta l}_n \cdot \hat{a}_R(\theta, \phi)]^{1/2}, \quad (15)$$

and

$$\vec{\delta l}_n = \frac{\vec{\Delta l}_n}{R} \quad (16)$$

If the phase, ϕ_n , is chosen to cancel r_n in some particular direction, say (θ_p, ϕ_p) , the array is focused at \vec{R}_p . If we assume that $\delta l_n \ll 1$, then

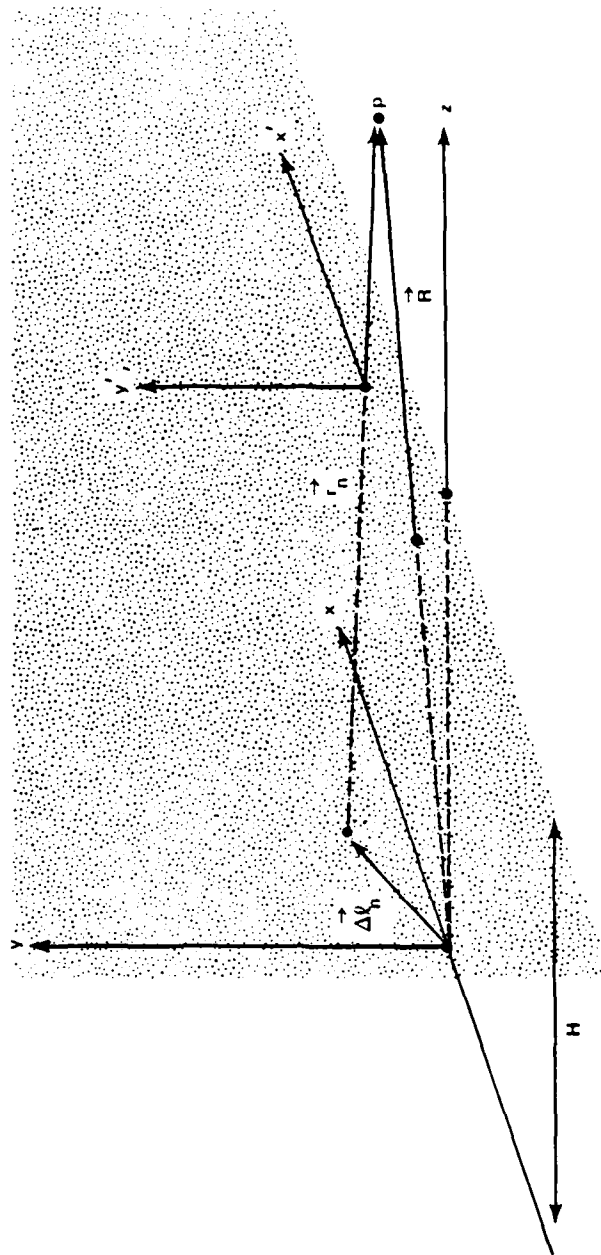


FIGURE 3 COORDINATE SYSTEM FOR ANALYSIS OF DISTRIBUTED SYSTEM

$$E_r(\theta, \phi) = \frac{\exp\{-ikR\}}{R} \sum_n A_n \exp\{-i[\phi_n - k\Delta_n(\theta, \phi)]\} \quad (17)$$

where

$$\Delta_n(\theta, \phi) = \frac{1}{2} |\vec{\delta l}_n|^2 - \vec{\delta l}_n \cdot \vec{a}_R(\theta, \phi) \quad (18)$$

The quadratic term in Eq. (18) is often neglected.

If a striated region is located at a distance, H , from the array plane, its effects can be formally accommodated in Eq. (5) by replacing A_n by $A_n h_n$ where h_n is a complex random variable. Because h_n is random, performance measures are derived by averaging quantities of interest. For example, the power pattern of the array can be computed as

$$\begin{aligned} P(\theta, \phi) &\triangleq R^2 \langle |E_R(\theta, \phi)|^2 \rangle \\ &= \sum_{n,m} A_n A_m \langle h_n h_m^* \rangle \exp\{i[(\phi_n - k\Delta_n) - (\phi_m - k\Delta_m)]\} \quad (19) \end{aligned}$$

To evaluate h_n , consider the wave propagating along the ray from $\vec{\delta l}_n$ to \vec{R} . Applying the Huygens-Fresnel formula,

$$\begin{aligned} h_n(\vec{\rho}_n, z_n) &= \iint \hat{u}(\vec{\kappa} + \vec{k}_{Tn}) \exp\left\{-iH_n(\vec{\kappa}) \frac{r_{en}}{2k}\right\} \\ &\quad \times \exp\{-i\vec{\kappa} \cdot \vec{\rho}_{sn} C_n\} \frac{d\vec{\kappa}}{(2\pi)^2} \quad (20) \end{aligned}$$

where the remaining parameters are defined as:

$$r_{en} = \frac{r_n^{(1)} r_n^{(2)}}{r_n^{(1)} + r_n^{(2)}} \quad (21a)$$

$$C_n = r_n^{(1)} / r_n \quad (21b)$$

$$H_n = \kappa^2 + (\kappa_x \cos \phi_n + \kappa_y \sin \phi_n)^2 \tan^2 \theta_n \quad (21c)$$

$$\vec{\rho}_{sn} = \vec{\rho}_n - \hat{a}_{r_{Tn}} z_n \tan \theta_n \quad (21d)$$

A derivation and discussion of Eq. (20) can be found in Reference 5. If Eq. (20) is substituted into $\langle h_n h_m^* \rangle$ and the orthogonal increments property of $\hat{u}(\vec{\kappa})$ --the Fourier spectrum of the wave as it emerges from the disturbed region--is applied, the result is

$$\begin{aligned} \langle h_n h_m^* \rangle = & \iint \langle \hat{u}(\vec{\kappa} + \vec{k}_{Tn}) \hat{u}^*(\vec{\kappa} + \vec{k}_{Tm}) \rangle \\ & \times \exp \left\{ -i \left[H_n \frac{r_{en}}{2k} - H_m \frac{r_{em}}{2k} \right] \right\} \\ & \times \exp \left\{ -i \vec{\kappa} \cdot (\vec{\rho}_{sn} C_n - \vec{\rho}_{sm} C_m) \right\} \frac{d\vec{\kappa}}{(2\pi)^2} \quad (22) \end{aligned}$$

With straightforward algebraic manipulations, it can be shown that

$$C_n = [1 - (H/R - \delta z_n) / (\cos \theta - \delta z_n)] \quad (23)$$

and

$$\rho_{sn} = r_n (1 - \sin \theta_n) (\cos \phi_n, \sin \phi_n) \quad (24)$$

where

$$\begin{bmatrix} \cos \phi_n \\ \sin \phi_n \end{bmatrix} = \sin \theta \begin{bmatrix} \cos \phi \\ \sin \phi \end{bmatrix} - \begin{bmatrix} \delta x_n \\ \delta y_n \end{bmatrix} D_n^{-1} \quad (25a)$$

and

$$D_n = \left[\sin^2 \theta + \delta x_n^2 + \delta y_n^2 - 2\delta l_n \cdot \hat{a}_{R_T} \sin \theta \right]^{1/2} \quad (25b)$$

For $R \gg \lambda$, the antenna beam width is such that δl_n is small compared to θ . Thus,

$$\begin{pmatrix} \cos \phi_n \\ \sin \phi_n \end{pmatrix} \cong \begin{pmatrix} \cos \phi \\ \sin \phi \end{pmatrix} ; \quad (26)$$

moreover, $\sin \theta_n \ll 1$, so that

$$\vec{\rho}_{sn} C_n - \vec{\rho}_{sm} C_m \cong \vec{\Delta l}_{nm} (1 - H \sec \theta / R) \quad , \quad (27)$$

where

$$\vec{\Delta l}_{nm} = \vec{\Delta l}_n - \vec{\Delta l}_m \quad (28)$$

is the vector between the n^{th} and m^{th} elements. A similar analysis shows that the propagation terms in Eq. (22) cancel and that $\vec{k}_{Tn} \sim \vec{k}_{Tm} \sim \vec{k}_T$.

It follows that

$$\begin{aligned} \langle h_n h_m^* \rangle &\cong \iint \langle |\hat{u}(\vec{k} + \vec{k}_T)|^2 \rangle \exp(-i\vec{k} \cdot \vec{\Delta l}_{nm} C) \frac{d\vec{k}}{(2\pi)^2} \\ &= \exp\{-\frac{1}{2} D_{\delta\phi}(\vec{\Delta l}_{nm} C)\} \quad , \end{aligned} \quad (29)$$

where $D_{\delta\phi}(\vec{\xi})$ is the phase structure function for the ray path along \vec{k} and

$$C = 1 - H \sec \theta / R \quad (30)$$

To summarize, the far-field voltage pattern for a cluster of non-interacting radiators with an intervening propagation disturbance is given by the expression

$$E_R(\theta, \phi) = \frac{\exp\{-ikR\}}{R} \sum_n A_n h_n \exp\{-i\delta \vec{l}_n \cdot \Delta \vec{K}\} \quad (31)$$

where

$$\Delta \vec{K} = k[\hat{a}_R(\theta, \phi) - \hat{a}_R(\theta_p, \phi_p)] \quad (32)$$

If the reference wave is omitted and the summation is converted to an integral, the integral expression in Eq. (10) results.

The model can be used for simulations or direct computations. As an example, we computed the average power pattern as defined by Eq. (19). Substituting Eq. (29) into Eq. (19), we have

$$\begin{aligned} P(\theta, \phi) &= \sum_{n,m} A_n A_m^* \exp\{-\frac{1}{2} D_{\delta\phi}(\Delta \vec{l}_{nm} C)\} \exp\{-i\Delta \vec{l}_{nm} \cdot \Delta \vec{K}\} \\ &\quad \iiint A(\vec{\rho}_1') A^*(\vec{\rho}_1'') \exp\{-D_{\delta\phi}(\Delta \vec{\rho}_1 C)\} \\ &\quad \times \exp\{-i\Delta \vec{\rho}_1 \cdot \Delta \vec{K}\} d\vec{\rho}_1' d\vec{\rho}_1'' \end{aligned} \quad (33a)$$

By changing the variable, Eq. (33a) can be written in the equivalent form

$$P(\theta, \phi) = \iint F(\Delta \vec{\rho}_1) \exp\{-\frac{1}{2} D_{\delta\phi}(\Delta \vec{\rho}_1 C)\} \exp\{-i\Delta \vec{\rho}_1 \cdot \Delta \vec{K}\} d\Delta \vec{\rho}_1 \quad (33b)$$

where

$$F(\Delta \vec{\rho}_1) = \iint A(\vec{x} + \Delta \vec{\rho}_1/2) A(\vec{x} - \Delta \vec{\rho}_1/2) d\vec{x} \quad . \quad (34)$$

In Section IV we shall evaluate Eq. (33) for a simple representative aperture distribution. The form of the structure function is derived from the SATCOM channel model.

III PROPAGATION EFFECTS OVER A TWO-WAY PATH

As discussed in Section I, a complete analysis of SBR propagation effects must accommodate the two-way path. As noted in Section I, the only effect of a source-receiver interchange is in the spherical wave correction factor [cf. Eqs. (2) and (5)]. For the distributed array analyzed in Section III, C as defined by Eq. (30) is replaced by

$$\begin{aligned} C_R &= 1 - C \\ &= H \sec \Theta/R \end{aligned} \quad (35)$$

If the target has scattering cross section, σ , it follows that the reflected signal at the antenna array described in Section II admits the representation

$$v_s(\Delta \vec{K}_0) = \sqrt{\sigma} \sum_n \sum_m A_n h_n A_m^R h_m^R \exp\{i(\delta \vec{l}_n + \delta \vec{l}_m) \cdot \Delta \vec{K}_0\} \quad (36)$$

where $\Delta \vec{K}_0$ is the wave vector for a target in the (Θ_0, ϕ_0) direction.

The return average power for a point reflector in the (Θ_0, ϕ_0) direction can be computed from the formula

$$\begin{aligned} \langle |v_A(\Delta \vec{K}_0)|^2 \rangle &= \sigma \sum_{n,n'} \sum_{m,m'} A_n A_{n'}^* A_m A_m^* \\ &\times \exp\{i(\delta \vec{l}_n - \delta \vec{l}_{n'}) \cdot \Delta \vec{K}_0\} \\ &\times \exp\{i(\delta \vec{l}_m - \delta \vec{l}_{m'}) \cdot \Delta \vec{K}_0\} \\ &\times \langle h_n h_{n'}^R, h_m h_{m'}^R \rangle \end{aligned} \quad (37)$$

The incident power and R^2 losses have been normalized to unity.

To evaluate the propagation term, we use Eq. (20) whereby

$$\begin{aligned}
\langle h_n h_n^{R*} h_m h_m^* \rangle = & \int \int \int \int \int \int \int \exp \{ -i [\vec{k}^{(1)} \cdot \vec{\rho}_n C^{(R)} - \vec{k}^{(2)} \cdot \vec{\rho}_{n,C}^{(R)} + \vec{k}^{(3)} \cdot \vec{\rho}_m C - \vec{k}^{(4)} \cdot \vec{\rho}_{m,C}] \} \\
& \times \exp \left\{ i [h(\vec{k}^{(1)}) - h(\vec{k}^{(2)}) + h(\vec{k}^{(3)}) - h(\vec{k}^{(4)})] \frac{z_p}{2k} \right\} \\
& \times \langle d\xi(\vec{k}^{(1)}) d\xi^*(\vec{k}^{(2)}) d\xi(\vec{k}^{(3)}) d\xi^*(\vec{k}^{(4)}) \rangle .
\end{aligned} \tag{38}$$

To evaluate Eq. (38), we make the following change of variables

$$2\vec{\alpha}^{(1)} = \vec{\rho}_n C^{(R)} + \vec{\rho}_{n,C}^{(R)} + \vec{\rho}_m C + \vec{\rho}_{m,C} \tag{39a}$$

$$2\vec{\alpha}^{(2)} = \vec{\rho}_n C^{(R)} - \vec{\rho}_{n,C}^{(R)} - \vec{\rho}_m C + \vec{\rho}_{m,C} \tag{39b}$$

$$2\vec{\alpha}^{(3)} = \vec{\rho}_n C^{(R)} + \vec{\rho}_{n,C}^{(R)} - \vec{\rho}_m C - \vec{\rho}_{m,C} \tag{39c}$$

$$2\vec{\alpha}^{(4)} = \vec{\rho}_n C^{(R)} - \vec{\rho}_{n,C}^{(R)} + \vec{\rho}_m C - \vec{\rho}_{m,C} . \tag{39d}$$

In the Fourier domain, we have

$$2\vec{q}^{(1)} = \vec{k}^{(1)} - \vec{k}^{(2)} + \vec{k}^{(3)} - \vec{k}^{(4)} \tag{40a}$$

$$2\vec{q}^{(2)} = \vec{k}^{(1)} + \vec{k}^{(2)} - \vec{k}^{(3)} - \vec{k}^{(4)} \tag{40b}$$

$$2\vec{q}^{(3)} = \vec{k}^{(1)} - \vec{k}^{(2)} - \vec{k}^{(3)} + \vec{k}^{(4)} \tag{40c}$$

$$2\vec{q}^{(4)} = \vec{k}^{(1)} + \vec{k}^{(2)} + \vec{k}^{(3)} + \vec{k}^{(4)} . \tag{40d}$$

Spatial homogeneity requires that Eq. (38) be independent of $\vec{\alpha}^{(1)}$. A necessary condition is that the fourth-order moment of the Fourier amplitudes must be a delta function in the $\vec{q}^{(1)}$ variable. It follows, therefore, after some algebraic manipulations that

$$\begin{aligned} \langle h_n^{(R)} h_{n'}^{(R)*} h_m h_m^* \rangle = \\ \iiint \exp\{-i[\vec{\alpha}^{(2)} \cdot \vec{q}^{(2)} + \vec{\alpha}^{(3)} \cdot \vec{q}^{(3)} + \vec{\alpha}^{(4)} \cdot \vec{q}^{(4)}]\} \\ \times \exp\{i\vec{q}^{(2)} \cdot \vec{q}^{(3)} \frac{z_p}{k}\} \phi_4(\vec{q}^{(2)}, \vec{q}^{(3)}, \vec{q}^{(4)}) \frac{d\vec{q}^{(2)}}{(2\pi)^2} \frac{d\vec{q}^{(3)}}{(2\pi)^2} \frac{d\vec{q}^{(4)}}{(2\pi)^2} \quad (41) \end{aligned}$$

In the spatial domain the equivalent expression is

$$\begin{aligned} \langle h_n^{(R)} h_{n'}^{(R)*} h_m h_m^* \rangle = \left(\frac{k}{2\pi z_p}\right)^2 \iiint M_4(\vec{\alpha}^{(2)} - \vec{\alpha}^{(2)''}, \vec{\alpha}^{(3)} - \vec{\alpha}^{(3)''}, \vec{\alpha}^{(4)}) \\ \times \exp\left\{-i\vec{\alpha}^{(2)''} \cdot \vec{\alpha}^{(3)''} \frac{k}{z_p}\right\} d\vec{\alpha}^{(4)''} d\vec{\alpha}^{(3)''} \quad (42) \end{aligned}$$

where

$$\vec{\alpha}^{(2)} = (\Delta \vec{\rho}_{nn}, C^{(R)} - \Delta \vec{\rho}_{mm}, C)/2 \quad (43a)$$

$$\vec{\alpha}^{(3)} = (\sum \vec{\rho}_{nn}, C^{(R)} - \sum \vec{\rho}_{mm}, C)/2 \quad (43b)$$

$$\vec{\alpha}^{(4)} = (\Delta \vec{\rho}_{nn}, C^{(R)} + \Delta \vec{\rho}_{mm}, C)/2 \quad (43c)$$

and $\Delta \vec{\rho}_{nn} = \vec{\rho}_n - \vec{\rho}_{n'}$, $\vec{\rho}_{nn} = \vec{\rho}_n + \vec{\rho}_{n'}$, etc. If $n = n'$ and $m = m'$, $\vec{\alpha}^{(2)} = \vec{\alpha}^{(4)} = 0$ and $\vec{\alpha}^{(3)} = \vec{\rho}_n C^{(R)} - \vec{\rho}_m C$. Finally, if $C^{(R)} = C$, Eq. (42) reduces to the equation for the intensity autocorrelation function used in Aino.^{3,4}

To evaluate M_4 , we use the Gaussian phase screen model, whereby

$$M_4(\vec{\alpha}_{(2)}, \vec{\alpha}_{(3)}, \vec{\alpha}_{(4)}) = \exp \left\{ - \left[D(\vec{\alpha}^{(2)} + \vec{\alpha}^{(4)}) - D(\vec{\alpha}^{(2)} + \vec{\alpha}^{(3)}) \right. \right. \\ \left. \left. + D(\vec{\alpha}^{(3)} + \vec{\alpha}^{(2)}) + D(\vec{\alpha}^{(2)} - \vec{\alpha}^{(4)}) \right. \right. \\ \left. \left. - D(\vec{\alpha}^{(2)} - \vec{\alpha}^{(3)}) + D(\vec{\alpha}^{(3)} - \vec{\alpha}^{(4)}) \right] \right\} \quad (44)$$

For a power-law phase screen with a one-dimensional spectral index less than 2, $D(\vec{\alpha}) \cong C_{\delta\phi}^2 |\alpha|^{2\nu-1}$ where $0.5 < \nu < 1.5$. When all the appropriate substitutions are made, it can be shown that

$$\langle h_n^R h_n^{R*} h_m^R h_m^{R*} \rangle = \iint \exp \left\{ - C_{\delta\phi}^2 \left[|\Delta \vec{\rho}_{nm}^R - \vec{\alpha}^{(2)}|^{2\nu-1} \right. \right. \\ \left. \left. + |\Delta \vec{\rho}_{nm}^R - \vec{\alpha}^{(2)}|^{2\nu-1} \right] \right\} \left(\frac{k}{2\pi z_p} \right)^2 \\ \times \iint \exp \left\{ - C_{\delta\phi}^2 \left[|\vec{\rho}_{nm}^R - \vec{\alpha}^{(3)}|^{2\nu-1} + |\vec{\rho}_{n'm}^R - \vec{\alpha}^{(3)}|^{2\nu-1} \right. \right. \\ \left. \left. - |\vec{\rho}_{nm}^R - \vec{\alpha}^{(2)} - \vec{\alpha}^{(3)}|^{2\nu-1} - |\vec{\rho}_{n'm}^R + \vec{\alpha}^{(2)} - \vec{\alpha}^{(3)}|^{2\nu-1} \right] \right\} \\ \times \exp \left\{ - i \vec{\alpha}^{(2)} \cdot \vec{\alpha}^{(3)} \frac{k}{z_p} \right\} d\vec{\alpha}^{(3)} d\vec{\alpha}^{(2)} \quad (45)$$

where $\vec{\rho}_{nm}^R = \vec{\rho}_n^R C^{(R)} - \vec{\rho}_m^R C$, etc.

When the phase structure constant, $C_{\delta\phi}^2$, is sufficiently large, the inner integral approximates $\delta(\vec{\alpha}^{(2)})$. To prove this formally, we first consider the behavior of the argument of the first exponential as $\alpha^{(3)} \rightarrow \infty$. By using an appropriate series expansion [Eq. (31) in Reference 3], we can show that the argument converges to zero (as long as $\nu < 1.5$) so that the exponential is near unity. For small values of $\alpha^{(3)}$, the contribution can always be reduced to a negligible value by increasing $C_{\delta\phi}^2$. In effect, the integral over $\vec{\alpha}^{(3)}$ is equivalent to the integral over the complex exponential, which is $\delta(\vec{\alpha}^{(2)})$. It follows that

$$\lim_{C_{\delta\phi}^2 \rightarrow \infty} \langle h_n^R h_n^{R*}, h_m^R h_m^{R*} \rangle \cong \exp \left\{ - C_{\delta\phi}^2 |\Delta \vec{\rho}_{nn}, C^{(R)}|^{2\nu-1} \right\} \\ \times \exp \left\{ - C_{\delta\phi}^2 |\Delta \vec{\rho}_{mm}, C|^{2\nu-1} \right\} \quad . \quad (46)$$

When Eq. (10) applies, Eq. (1) becomes

$$|V_A(\Delta \vec{K}_0)|^2 = \sigma \left(\sum_{nn'} A_n A_n^* \langle h_n^R h_n^{R*} \rangle \exp \{ i(\delta \vec{\ell}_n - \delta \vec{\ell}_{n'}) \cdot \Delta \vec{K}_0 \} \right) \\ \times \left(\sum_{mm'} A_m A_m^* \langle h_m^R h_m^{R*} \rangle \exp \{ i(\delta \vec{\ell}_m - \delta \vec{\ell}_{m'}) \cdot \Delta \vec{K}_0 \} \right) \quad . \quad (47)$$

That is, the power received can be computed from the product of the average transmit and received antenna patterns, just as it is for an undisturbed path.

The analysis presented in this section verifies that under the same conditions the intensity scintillation satisfies the Rayleigh relationship

$$\langle II' \rangle - 1 \approx |\langle vv'^* \rangle|^2 \quad (48)$$

where $I = |v|^2$, the forward and reciprocal radar paths are uncorrelated. This has proven to be a very durable relationship for naturally occurring scintillation with S_4 near unity. Thus, based on the special case analyzed in this section and the more extensive experimental results, it seems safe to use Eqs. (8) and (9) as a basis for analysis and simulations of SBR propagation effects.

IV APPLICATIONS OF THE MODEL

To illustrate the use of the model, we shall evaluate Eq. (34) for the Gaussian aperture distribution function

$$A(\vec{\rho}) = \exp\{-\rho^2/2r_0^2\} \quad . \quad (49)$$

The result is

$$F(\vec{\rho}) = \pi r_0^2 \exp\{-\rho^2/(4r_0^2)\} \quad . \quad (50)$$

A gaussian aperture cannot be realized because it has no sidelobes; however, it can be used to estimate the distortion of the main beam if an appropriate definition of the aperture cutoff, r_0 , is used.

To complete the model specification, we must define the mutual coherence function or, equivalently, the phase structure function $D_{\delta\phi}(\vec{\xi})$. The general form of $D_{\delta\phi}(\vec{\xi})$ is unwieldy; thus, approximations must be used. For example, in the power-law regime where the three-dimensional spectral density function has the form

$$\phi(K) = C_s q^{-(2+1)} \quad , \quad (51)$$

the structure function admits a similar power-law representation

$$D_{\delta\phi}(\Delta\vec{\rho}) = C_{\delta\phi}^2 y^{\min[2\nu-1, 2]} \quad (52)$$

where $C_{\delta\phi}^2$ is the phase structure constant. This is discussed in Rino.⁵ The anisotropy of wave field is accommodated by taking

$$y = \left[\frac{C' \Delta \rho_x^2 - B' \Delta \rho_x \Delta \rho_y + A' \Delta \rho_y^2}{A' C' - B'^2/4} \right]^{1/2} \quad (53)$$

Wittwer^{2,6} has developed a complete signal specification for evaluating radiowave propagation disturbances. Equation (25) in his 1979 report is equivalent to Eqs. (52) and (53) for $\nu = 1.5$. A parallel development for ionospheric applications is described in Reference 5 and the references cited therein. Table 1 summarizes the notations used in the two developments.

For data interpretation, we have found it convenient to use the structure and phase turbulent strength parameters, C_s and

$$C_p = r_e^2 \lambda^2 l_p C_s G \quad (54)$$

where $r_e (= 2.87 \times 10^{-15} \text{ m})$ is the classical electron radius, λ is the wavelength, and l_p is the propagation path length. On the other hand, most other analyses are specified in terms of the rms electron density, $\langle \Delta N_e^2 \rangle^{1/2}$, and the rms phase, $\sigma_{\delta\phi}$. The interrelationships are given by the formulas,

$$C_s = 8\pi^{3/2} q_o^{2\nu-2} \frac{\Gamma(\nu+1/2)}{\Gamma(\nu-1)} \langle \Delta N_e^2 \rangle \quad , \quad (55)$$

and

$$C_p = q_o^{2\nu-1} \frac{\Gamma(\nu+1/2)}{\Gamma(\nu-1/2)} \sigma_{\delta\phi}^2 \quad . \quad (56)$$

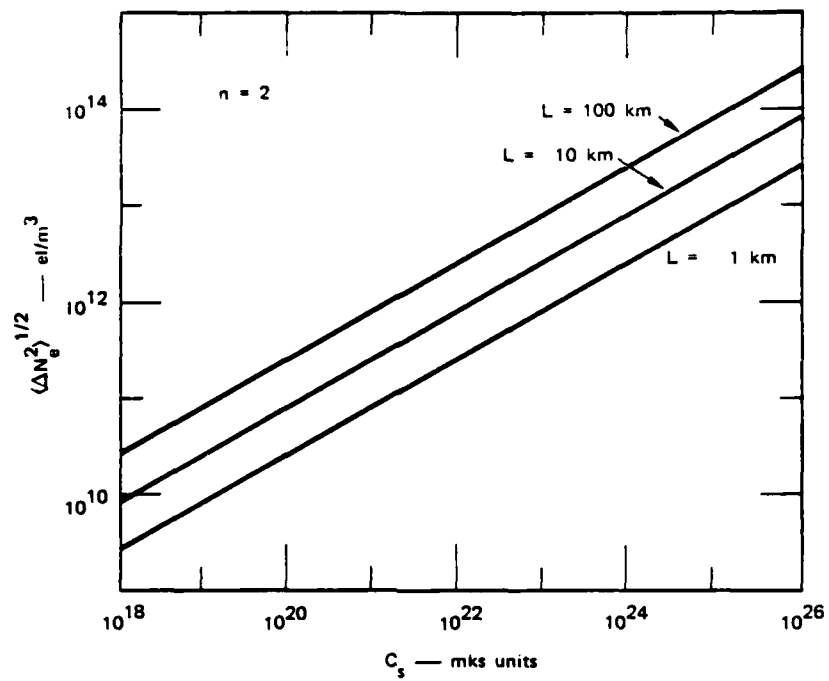
Plots of $\langle \Delta N_e^2 \rangle$ versus C_s and $\sigma_{\delta\phi}$ versus C_p for $\nu = 1.5$ are given in Figures 4(a) and 4(b).

Table 1
NOTATION FOR PROPAGATION MODELING

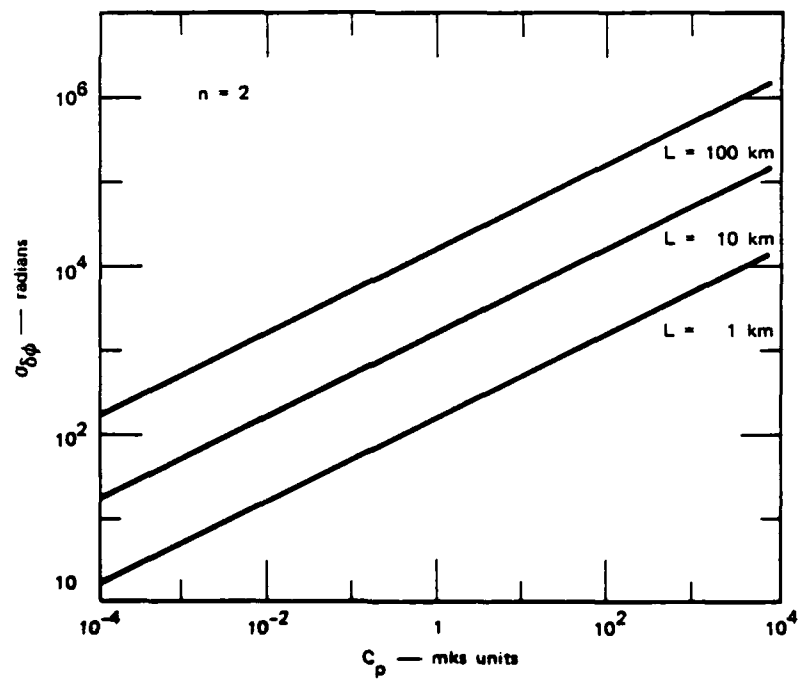
Natural Ionosphere	Wittwer	Comment
q_o	L_s^{-1}	Outer scale wavenumber
a	L_t/L_s	Axial ratio along field
b	L_r/L_s	Transverse axial ratio
δ	θ	Orientation of transversal irregularity axis
G	$q_o L_z$	Geometric enhancement factor
ψ_{BP}^{\dagger}	ϕ	Briggs-Parkin angle
aq_o/G	$L_u = L_s^2(a^2 \cos^2 \phi + \sin^2 \phi)$	Briggs-Parkin factor
θ		Zenith angle
φ		Magnetic azimuth angle
$z_R \sec \theta$	$z_f = \frac{(z_T - z_l)z_l}{z_T}$	"Reduced" propagation distance
ν	$n = \nu + \frac{1}{2}$	Spectral index parameter
$\phi_{\Delta N_e} \sim q^{-(2\nu+1)}$	$\phi_{\Delta N_e} \sim q^{2n}$	Form of three-dimensional spectral density function

[†]The Briggs-Parkin angle--the angle between the line-of-sight and the magnetic field--is given in terms of ψ , θ , and φ as

$$\cos \psi_{BP} = \cos \psi \sin \theta \cos \varphi + \sin \psi \cos \theta$$



(a) IN SITU



(b) PHASE

FIGURE 4 CONVERSION OF rms MEASURES TO TURBULENT STRENGTHS

A good approximation to $C_{\delta\phi}^2$ is given by the formula

$$C_{\delta\phi}^2 = \frac{C_D}{2\pi} (v^2 - 4.5v + 5.5) \quad 1 \leq v \leq 2, \quad (57)$$

which is essentially equivalent to Eq. (23) in Wittwer.⁶ If we take $v = 1.5$ as representative, Eq. (33) is readily evaluated as

$$P(\theta_A, \phi_A) = \frac{4(\pi r_o^2)^2}{\mathcal{A} - \mathcal{B}^2/4} \exp \left\{ -r_o^2 [\mathcal{A} \Delta K_x^2 + \mathcal{B} \Delta K_x \Delta K_y + \mathcal{C} \Delta K_y^2] \right\} \quad (58)$$

where

$$\mathcal{A} = 1 + 4 \left(\frac{r_o}{\ell_o C} \right)^2 \left(\frac{A}{A C - B^2/4} \right) \quad (59a)$$

$$\mathcal{B} = 4 \left(\frac{r_o}{\ell_o C} \right)^2 \left(\frac{B'}{A' C' - B'^2/4} \right) \quad (59b)$$

$$\mathcal{C} = 1 + 4 \left(\frac{r_o}{\ell_o C} \right)^2 \left(\frac{C'}{A' C' - B'^2/4} \right) \quad (59c)$$

and

$$\ell_o = [C_{\delta\phi}^2]^{-1}. \quad (60)$$

We have assumed that the beam is focused on axis.

It is readily shown that as $\ell_o \rightarrow \infty$, $\mathcal{B} \rightarrow 0$ and $\mathcal{A} \rightarrow \mathcal{C} \rightarrow 1$. Thus, for small perturbations, there is no distortion of the average antenna pattern. As ℓ_o decreases, however, the beam is broadened and its

symmetry destroyed. As noted in Section I, the main parameter is the ratio of the spatial coherence scale, ℓ_o , to the aperture size.

To accommodate the temporal structure of the signal as well as beam spreading, $\Delta \vec{\rho}_\perp$ in Eq. (33b) need only be replaced by $\Delta \vec{\rho}_\perp - \vec{v}_\perp \delta t$. Again, with $v = 1.5$ the integral can be evaluated analytically as

$$\begin{aligned} \langle v_R v_R'^* \rangle &= P(\theta_A, \phi_A) R_h(\delta t) \exp\{-2 \cdot \vec{n} \cdot \Delta \vec{K} \delta t\} \\ &\times \exp\{-(r_o/\ell_o)^4 (v_{\text{eff}} \delta t)^2\} \end{aligned} \quad (61)$$

where the vector \vec{n} is given by the expression

$$\begin{pmatrix} n_x \\ n_y \end{pmatrix} = \frac{(r_o/\ell_o)^2}{AB - B^2/4} \begin{pmatrix} C & B/2 \\ B/2 & A \end{pmatrix} \begin{pmatrix} v_{Ex} \\ v_{Ey} \end{pmatrix} \quad (62)$$

For many applications, $r_o/\ell_o \ll 1$, and the "aperture smearing" terms in Eq. (42) can be neglected. Thus, on a one-way path the antenna pattern and temporal coherence functions are multiplicative; moreover, the multiplicative property is not upset if frequency coherence loss is accommodated as well. In effect, for $v = 1.5$ the SATCOM channel model can easily be modified to predict the complex signal coherence on a one-way path. For a two-way path, we need only replace C in Eq. (59) by the corresponding value for the reciprocal path and multiply the two coherence functions.

The analytic form presented here should be used with caution, however, because of the assumed Gaussian aperture distribution function. For the more exacting system analyses, a simulation based on the model described in Section II should be used.

REFERENCES

1. R. H. Hardin and F. D. Tappert, "Analysis, Simulation, and Models of Ionospheric Scintillation," Contract DAHC60-71-C-0005, Bell Laboratories/Western Electric (March 1974).
2. L. A. Wittwer, "A Trans-Ionospheric Signal Specification for Satellite C³ Applications," In-House Report, DNA 5662D, Defense Nuclear Agency, Washington, DC (December 1980).
3. J. D. Kraus, Radio Astronomy, Chap. 6 (McGraw-Hill, New York, NY, 1966).
4. C. L. Rino, "A Power-Law Phase Screen Model for Ionospheric Scintillation 2. Strong Scatter," Radio Science, Vol. 14, No. 6, p. 1147 (1979).
5. C. L. Rino, "Numerical Computations for a One-Dimensional Power-Law Phase Screen," Radio Science, Vol. 15, p. 41 (1980).
6. C. L. Rino, "Propagation Modeling and Evaluation of Communication System Performance in Nuclear Environments," Final Report, Contract DNA-001-77-C-0038, SRI Project 5960, SRI International, Menlo Park, CA (February 1980).
7. L. A. Wittwer, "Radio Wave Propagation in Structured Ionization for Satellite Applications," In-House Report, DNA 5304D, Defense Nuclear Agency, Washington, DC (December 1979).

DISTRIBUTION LIST

DEPARTMENT OF DEFENSE

Command & Control Technical Center

ATTN: C-650

3 cy ATTN: C-650, W. Heidig

Defense Communications Agency

ATTN: Code 230

ATTN: Code 205

ATTN: J300 for Yen-Sun Fu

Defense Communications Engineer Center

ATTN: Code R410, N. Jones

ATTN: Code R410

ATTN: Code R410, R. Craighill

ATTN: Code R123

Defense Nuclear Agency

ATTN: STNA

ATTN: NAFD

ATTN: RAEF

ATTN: NATD

ATTN: RAAE, P. Lunn

3 cy ATTN: RAAE

4 cy ATTN: TITL

Defense Technical Information Center

12 cy ATTN: DD

Dep Under Secretary of Defense

Comm, Cmd, Cont & Intell

ATTN: Dir of Intelligence Sys

Field Command

Defense Nuclear Agency, Det 1

Lawrence Livermore Lab

ATTN: FC-1

Interservice Nuclear Weapons School

ATTN: TTV

WMCCS System Engineering Org

ATTN: J. Hoff

DEPARTMENT OF THE ARMY

BMD Advanced Technology Center

ATTN: ATC-R, D. Russ

ATTN: ATC-O, W. Davies

ATTN: ATC-R, W. Dickinson

ATTN: ATC-T, M. Capps

BMD Systems Command

ATTN: BMDSC-HLE, R. Webb

2 cy ATTN: BMDSC-HW

Harry Diamond Laboratories

ATTN: DELHD-NW-P

ATTN: DELHD-NW-R, R. Williams

US Army Communications Command

ATTN: CC-OPS-W

ATTN: CC-OPS-WR, H. Wilson

DEPARTMENT OF THE ARMY (Continued)

US Army Foreign Science & Tech Ctr

ATTN: DRXST-SD

US Army Nuclear & Chemical Agency

ATTN: Library

DEPARTMENT OF THE NAVY

Naval Electronic Systems Command

ATTN: PME 117-211, B. Kruger

ATTN: PME 106-13, T. Griffin

ATTN: Code 501A

ATTN: PME 117-20

ATTN: PME 117-2013, G. Burnhart

ATTN: Code 3101, T. Hughes

ATTN: PME 106-4, S. Kearney

Naval Ocean Systems Center

ATTN: Code 5322, M. Paulson

ATTN: Code 532

ATTN: Code 5323, J. Ferguson

Naval Research Laboratory

ATTN: Code 4720, J. Davis

ATTN: Code 4780

ATTN: Code 7500, B. Wald

ATTN: Code 4780, S. Ossakow

ATTN: Code 6700

ATTN: Code 7950, J. Goodman

ATTN: Code 4187

ATTN: Code 4700

Naval Space Surveillance System

ATTN: J. Burton

Naval Surface Weapons Center

ATTN: Code F31

Office of Naval Research

ATTN: Code 412, W. Condell

ATTN: Code 414, G. Joiner

Theater Nuclear Warfare Proj Office

ATTN: PM-23, D. Smith

DEPARTMENT OF THE AIR FORCE

Aerospace Defense Command

ATTN: DC, T. Long

Air Force Geophysics Laboratory

ATTN: OPR, H. Gardiner

ATTN: OPR-1

ATTN: LKB, K. Champion

ATTN: CA, A. Stair

ATTN: PHY, J. Buchau

ATTN: R. Babcock

ATTN: R. O'Neill

Air Force Technical Applications Ctr

ATTN: TN

DEPARTMENT OF THE AIR FORCE (Continued)

Air Force Weapons Laboratory

ATTN: SUL
ATTN: NTYC
ATTN: NTN

Air Force Wright Aeronautical Lab

ATTN: A. Johnson
ATTN: W. Hunt

Air University Library

ATTN: AUL-LSE

Assistant Chief of Staff
Studies & Analyses

ATTN: AF/SASC, C. Rightmeyer
ATTN: AF/SASC, W. Kraus

DEPARTMENT OF ENERGY CONTRACTOR

Sandia National Lab

ATTN: D. Dahlgren
ATTN: Tech Lib 3141
ATTN: Space Project Div
ATTN: D. Thornbrough
ATTN: Org 1250, W. Brown
ATTN: Org 4231, T. Wright

DEPARTMENT OF DEFENSE CONTRACTORS

Aerospace Corp

ATTN: V. Josephson
ATTN: T. Salmi
ATTN: R. Slaughter
ATTN: I. Garfunkel
ATTN: J. Straus
ATTN: D. Olsen

Analytical Systems Engineering Corp

ATTN: Radio Sciences

BDM Corp

ATTN: L. Jacobs
ATTN: T. Neighbors

Berkeley Research Associates, Inc

ATTN: J. Workman
ATTN: S. Brecht
ATTN: C. Prettie

EOS Technologies, Inc

ATTN: B. Gabbard

ESL, Inc

ATTN: R. Ibaraki
ATTN: R. Heckman
ATTN: J. Lehman
ATTN: E. Tsui
ATTN: J. Marshall

General Research Corp

ATTN: B. Bennett

Geo-Centers, Inc

ATTN: E. Marram

Honeywell, Inc

ATTN: G. Collyer, Avionics Dept
ATTN: G. Terry, Avionics Dept

DEPARTMENT OF DEFENSE CONTRACTORS (Continued)

Kaman Sciences Corp

ATTN: T. Stephens

Kaman Tempo

ATTN: B. Gambill
ATTN: DASIAC
ATTN: J. Devore
ATTN: W. Knapp
ATTN: K. Schwartz
ATTN: W. McNamara

M.I.T. Lincoln Lab

ATTN: D. Towle

Mission Research Corp

ATTN: R. Hendrick
ATTN: C. Lauer
ATTN: R. Kilb
ATTN: F. Fajen
ATTN: R. Bigoni
ATTN: G. McCartor
ATTN: F. Guigliano
ATTN: Tech Library
ATTN: S. Gutsche
ATTN: R. Bogusch

Mitre Corp

ATTN: A. Kymmel
ATTN: B. Adams
ATTN: G. Harding
ATTN: C. Callahan
ATTN: MS J104/M, R. Dresch

Mitre Corp

ATTN: W. Hall
ATTN: M. Horrocks
ATTN: W. Foster
ATTN: J. Wheeler

Pacific-Sierra Research Corp

ATTN: F. Thomas
ATTN: E. Field, Jr
ATTN: H. Brode, Chairman SAGE

Pennsylvania State University

ATTN: Ionospheric Research Lab

Photometrics, Inc

ATTN: I. Kofsky

Physical Dynamics, Inc

ATTN: E. Fremouw

Physical Research, Inc

ATTN: R. Deliberis

R&D Associates

ATTN: R. Lelevier
ATTN: C. Greifinger
ATTN: R. Turco
ATTN: H. Ory
ATTN: W. Wright
ATTN: M. Gantsweg
ATTN: W. Karzas
ATTN: F. Gilmore

R&D Associates

ATTN: B. Yoon

DEPARTMENT OF DEFENSE CONTRACTORS (Continued)

SRI International

ATTN: G. Price
ATTN: R. Tsunoda
ATTN: J. Vickrey
ATTN: W. Chesnut
ATTN: R. Livingston
ATTN: D. Neilson
ATTN: D. McDaniels
ATTN: R. Leadabrand
ATTN: M. Baron
ATTN: A. Burns
ATTN: G. Smith
ATTN: V. Gonzales
ATTN: W. Jaye
ATTN: J. Petrickes

4 cy ATTN: C. Rino

DEPARTMENT OF DEFENSE CONTRACTORS (Continued)

Rand Corp

ATTN: E. Bedrozian
ATTN: C. Crain

Sylvania Systems Group

ATTN: J. Concordia
ATTN: I. Kohlberg

Visidyne, Inc

ATTN: C. Humphrey
ATTN: O. Shepard
ATTN: W. Reidy
ATTN: J. Carpenter